Atmos. Chem. Phys. Discuss., 9, 12927–12963, 2009
www.atmos-chem-phys-discuss.net/9/12927/2009/

Atmospheric Chemistry and Physics Discussions

This discussion paper is/has been under review for the journal *Atmospheric Chemistry and Physics (ACP)*. Please refer to the corresponding final paper in *ACP* if available.

Theoretical implication of reversals of the ozone weekend effect systematically observed in Japan

A. Kannari[1] **and T. Ohara**[2]

[1]Independent researcher, NIES visiting researcher, Tokyo, Japan
[2]National Institute for Environmental Studies (NIES), Tsukuba, Japan

Received: 20 May 2009 – Accepted: 1 June 2009 – Published: 8 June 2009

Correspondence to: A. Kannari (kannari.akiyoshi@circus.ocn.ne.jp)

Published by Copernicus Publications on behalf of the European Geosciences Union.

Abstract

Systematic changes of the ozone weekend effect are found over broad areas of Japan. These changes are characterized by (1) spatial reversals from a weekend increase in the vicinity of huge precursor source areas to a weekend decrease in the surrounding rural areas, and (2) temporal reversals from a weekend increase under relatively unsuitable meteorological conditions for ozone formation to a weekend decrease under relatively suitable conditions. We developed a simple numerical advection-reaction model to explain the relationship between the duration of advection and the supplied solar energy, which causes the daily maximum ozone concentration to be lower near the precursor source. Ozone isopleth diagrams for individual advection durations (equivalent to the distance from the source) for a wide range of initial precursor conditions show that both VOC-limited and NO_x-limited regimes exist for each advection duration, but the area of NO_x-limited regime becomes dominant as the advection duration increases because of the increased exposure of the air mass to solar energy. For given initial VOC and NO_x concentrations, the area remote from the source becomes a NO_x-limited regime even if the precursor source area is in the VOC-limited regime. The rate of reduction of weekend emissions of NO_x is larger than that of VOC, causing a weekend increase in a VOC-limited regime near the source, but a weekend decrease in remote areas with a NO_x-limited regime. The boundary between these two ozone formation regimes depends on meteorological conditions: when sunlight intensity and temperature are relatively low, the change from a VOC-limited to a NO_x-limited regime occurs at a point more remote from the source than when they are relatively high, which causes a prevailing ozone weekend increase over a wide geographical area on days with lower ozone potential. Therefore, observations of ozone weekend changes can be interpreted in light of the theoretical implications of our model; they can be used for determination of ozone formation regimes, which change in different locations and under different meteorological conditions.

ACPD

9, 12927–12963, 2009

1 Introduction

Many observational studies have found weekend ozone concentration changes in large cities and their surroundings over the past 30 years. The most remarkable and frequently observed phenomenon is a rise in ozone concentrations on the weekend despite a weekend decrease in the emissions of ozone precursors (the "weekend effect"). This weekend effect has been observed in many cities around the world since the 1970s (e.g., Cleveland et al., 1974; Elkus and Wilson, 1977; Altshuler et al., 1995; and many other studies cited by Stephens et al., 2008). In general, the ozone weekend effect is thought to reflect a larger weekend reduction in NO_x emissions than in non-methane volatile organic compound (NMVOC, hereinafter simply called the "VOC") emissions. The most probable, though not yet well established, cause of a weekend increase in ozone levels, among the six hypotheses suggested by the California Air Resource Board, is a larger reduction in NO_x emissions than in emissions of VOCs in a VOC-limited ozone formation regime (Heuss et al., 2003).

Two recent findings concerning the ozone weekend effect are particularly important. First, a spatial reversal of the ozone weekend effect, from a weekend increase near the precursor source area to a weekend decrease in downwind rural areas, has been reported (Blanchard and Fairley, 2001; Murphy et al., 2006). Second, a temporal reversal of the ozone weekend effect occurs at the same observation point, depending on the meteorological conditions: a weekend increase under relatively unsuitable meteorological conditions for ozone formation reverses to a weekend decrease under more suitable conditions (higher solar intensity and higher temperatures) (Brönnimann and Neu, 1997; Paschalidou and Kassomenos, 2004). These findings suggest that weekend changes in ozone concentrations reflect dynamic phenomena closely related to chemical transport mechanisms.

Kannari (2006a, b) studied observational data obtained by continuous monitoring from two metropolitan areas, Tokyo and Osaka-Kyoto, Japan, and found, by a detailed statistical analysis, both spatial and temporal systematic reversals of the ozone week-

ACPD
9, 12927–12963, 2009

end effect. The present study extends this analysis of the ozone weekend effect to broader areas in Japan. Moreover, Kannari and Ohara (2009) recently developed a simple theoretical model to concisely explain the mechanisms behind these systematic reversals of the ozone weekend effect. According to this model, the ozone formation regime changes with both distance from the precursor source and sunlight intensity, and these regime changes cause the reversals of the ozone weekend effect. In this paper, in light of the theoretical implications of our model, we discuss the usefulness of the observation of reversals of the ozone weekend effect for determination of ozone formation regimes.

2 Observed reversals of the ozone weekend effect

2.1 Observation data

In a cooperative research project, the National Institute for Environmental Studies and the many local governmental institutes for environmental studies in Japan have developed a historical data archive of hourly monitored data consisting of the concentrations of many air pollutants and observed meteorological parameters for 1972–2004. In our study, we used the hourly data for O_3, NO+NO_2 (NO_x), NMHC (hereinafter VOC, because the measured concentrations partly include oxygenated compounds), and surface meteorological parameters (wind, temperature, humidity, and solar radiation). We defined a valid day of ozone measurement as measurement over 12 or more hours between 05:00 and 20:00 local time (LT). Similarly, valid days of NO_x and VOC measurement are defined as a day with available measurement over 20 or more hours per day. Valid monitoring sites are defined as those with 250 or more valid measurement days annually. For our analyses, we used monitoring sites on the Japanese mainland (Honshu) and on Shikoku and Kyushu islands judged to be valid in every year from 1999 to 2004: 899 monitoring sites for O_3, 251 sites for VOC, and 1015 sites for NO_x.

ACPD
9, 12927–12963, 2009

2.2 Weekend changes in precursor concentrations

We classified all days as weekdays (Monday to Friday, excluding national holidays), Saturdays, or Sundays. We compared mean daytime (05:00–15:00 LT) concentrations of NO_x and VOC at the individual sites over the entire study period (1999–2004) between weekdays and Sundays (Fig. 1). Because Saturday is not a full holiday in Japan, precursor concentrations on Saturdays fall between those for weekdays and Sundays (data not shown). Mean daytime concentrations of NO_x decreased by almost 50% on Sundays, whereas VOC concentrations decreased by only about 20%. Therefore, the VOC/NO_x ratio significantly increased on Sundays by more than 40% (Fig. 1c). These findings agree with those reported in the United States (Blanchard and Fairley, 2001; Pun and Seigneur, 2003; Fijita et al., 2003). We consider this increase in VOC/NO_x to be a key factor in the ozone weekend change. The main cause of the weekend imbalance between NO_x and VOC is that most heavy-duty diesel trucks, which emit large amounts of NO_x but not very large amounts of VOCs, do not operate on Sundays in urban areas.

2.3 Reversals of the ozone weekend effect

We compared cumulative frequency curves of the daily maximum ozone concentration ($O_{3\,max}$) at each monitoring site between weekdays and Sundays (Fig. 2a). By comparing $O_{3\,max}$ between weekdays and Sundays at the same percentile rank, we ensured that we were comparing values under similar meteorological conditions (see Fig. 4c and d). Weekend changes in $O_{3\,max}$ at all 899 monitoring sites are shown in Fig. 2b. The ratio of weekend (Sunday) $O_{3\,max}$ to weekday values (colored scale) remarkably changes with the percentile rank; namely, most monitoring sites show a change from a weekend increase at lower percentile ranks to a weekend decrease at higher percentile ranks.

To investigate the cause of this systematic change in the ozone weekend effect, we examined the geographical distribution of Sunday/weekday $O_{3\,max}$ ratios at each

ACPD
9, 12927–12963, 2009

percentile rank. Figure 3a–d shows the example of spatial structure of the changes in the ozone weekend effect under the meteorological conditions for 70th~98th percentile rank of $O_{3\,max}$, respectively. For comparison, the spatial distributions of NO_x and VOC emission fluxes from 06:00 to 15:00 LT in July 2000 (Kannari et al., 2007) are shown in Fig. 3e and f. The VOC emission flux values include the flux from biogenic sources. Our study area included three metropolitan areas, Tokyo, Nagoya, and Osaka-Kyoto, each of which is an area of very high precursor emissions. At percentile ranks below the 70th percentile, only 2% of the monitoring sites show a weekend decrease more than 5% in ozone (Figs. 2b, 3a), but at the 80th percentile rank, areas remote from the high precursor emission sources show a weekend ozone decrease (Fig. 3b); moreover, at the 90, 98th percentile rank, even areas near the precursor source areas show a weekend decrease (Fig. 3c, d).

Both a spatial structure of the ozone weekend effect related to distance from the source areas, as described by Blanchard and Fairley (2001) and Murphy et al. (2006), and systematic changes in the weekend effect in relation to meteorological conditions, as reported by Brönnimann and Neu (1997) and Paschalidou and Kassomenos (2004), are apparent in Figs. 2 and 3. We therefore investigated emissions and meteorological conditions in greater detail in the Tokyo Metropolitan Area (TMA in Fig. 3a) (Fig. 4). We defined the regional ozone level in the TMA for each day as the average of the mean $O_{3\,max}$ in all 10 km×10 km grid cells. Figure 4a shows the percentage of monitoring sites showing a weekend increase (R>1.0) or a large weekend increase (R>1.1), where $R=O_{3\,max,Sunday}/O_{3\,max,weekday}$ in relation to the percentile rank of the regional ozone level. The number of sites showing a weekend increase dropped at higher regional ozone levels, consistent with the data shown in Fig. 2. Moreover, meteorological conditions (i.e., solar radiation and temperature) were clearly correlated with the percentile rank of the regional ozone concentration (Fig. 4c, d), suggesting that the changes in the ozone weekend effect with the ozone level were caused by changes in meteorological conditions, as has already been shown by Paschalidou and Kassomenos (2004).

ACPD
9, 12927–12963, 2009

Importantly, VOC/NO_x between 06:00 and 09:00 LT, calculated using data from the 180 sites monitoring both VOC and NO_x, showed a clear increase on Sundays relative to weekdays, and also gradually increased with the percentile rank of the regional ozone level (Fig. 4b).

In the TMA, when the regional ozone level is extremely high, surface wind system consists of a large scale sea breeze during the daytime, both on weekdays and Sundays (Fig. 5). Therefore, we inferred that the spatial changes in the ozone weekend effect shown in Fig. 3d occurred along the transport path from this large precursor source area, in a manner similar to the transport from the west coast to inland areas in central California shown by Blanchard and Fairley (2001).

These indirect lines of evidence suggest that the reversals of the ozone weekend effect shown in Figs. 2 and 3 essentially reflect spatial changes during chemical transport and are strongly affected by meteorological conditions. Kannari and Ohara (2009) explained the mechanism of spatial changes in the ozone weekend effect in relation to meteorological conditions by a very simple theoretical model. In the next section, we describe the main points of this model and its application to our data.

3 Analysis of the ozone weekend effect based on ozone isopleth diagrams

3.1 Advection-reaction model

Lagrangian-type photochemical models such as those based on the empirical kinetic modeling approach (e.g., Carter et al., 1982) are capable of predicting the highest ozone concentrations in an air mass once that air mass has moved away from the source. However, to investigate the mechanism of the spatial reversal of the ozone weekend effect, we must estimate daily maximum ozone concentrations at individual measurement points at different distances from the source. For this purpose, we developed a simple advection-reaction model (Kannari and Ohara, 2009). This model incorporates photochemical reactions that occur during advection only, for simplicity

excluding diffusion and deposition. In this paper, we use this model with minor modifications.

In the model, an air mass which starts from an up-wind edge of a source area continues to acquire precursor gases at a constant rate in the source area, and reactions occur continuously during its advection from its start point to the receptor both in the urban and rural area. The normalized distance (D) from the up-wind edge of source is defined as $D=X/U$, where X is the distance from the start point and U is wind speed. The length of source area is also defined by passing duration L (h) with uniform injection rate q (ppb/h) of precursors, and then supplied amounts of precursors are expressed as initial concentrations qL (ppb). The ozone concentration of the air mass passing the receptor at time T is estimated by estimating the photochemical reactions occurring from the release time (T–D) until the arrival time T. For a second arrival time T', the concentration is estimated independently by estimating the photochemical reactions occurring from (T'–D) until T'. Therefore, if a steady-state emission source is assumed, we can estimate changes in the ozone concentration at D independently for each individual air mass released at different times, as shown schematically in Fig. 6. The most important parameters in the model are the daily changes in solar radiation and temperature; therefore, according to the advection-reaction model, the maximum ozone concentration occurs at the time of day when solar radiation and temperature are highest during the advection (shown by the open circles in the figure). Consequently, at a point close to the source, the air mass that is released at a little before noon and arrives at a little after noon brings the highest ozone concentration ($O_{3\,max}$). At a point remote from the source, however, $O_{3\,max}$ is carried by an air mass that is released at an earlier time and arrives at a later time compared with the point close to the source. Thus, if there is not diffusion during the advection, the ozone concentration is always higher at remote points than at closer points because of the longer advection time and hence the longer time available for chemical reaction.

For the model analysis, we used averaged diurnal patterns of meteorological conditions, solar radiation, temperature, and humidity, over several percentile rank intervals

ACPD
9, 12927–12963, 2009

of the TMA ozone level (e.g. Fig. 7). We used the carbon bond IV (CBIV) chemical reaction scheme (Gery et al., 1989). We estimated VOC compositions (Table 1) from source-specific emissions in August 2000 in the area enclosed by the rectangle in Fig. 3f, as reported in the emission inventory EAGrid2000-Japan (Kannari et al., 2007), and the speciation profiles for each source. VOC compositions may differ between weekdays and weekends, but because we did not have weekend emission inventory data except for road vehicles, we used the overall composition by the mean emission rates. Source length of precursors was set to L=2 h, corresponding to ca. 20~40 km with 3~6 m/s of wind speed. Because precursors' emissions before 07:00 LT are very low in the TMA, we assumed constant rate emissions beginning at this time. This constraint affects to the $O_{3\,max}$ only at extremely remote point transported by over 10 h advection. In the model, NO_x is emitted as NO, 1 ppb is used as the initial ozone concentration, and 10^{-13} ppb as the initial concentration of all other species.

3.2 Ozone isopleth diagrams

Isopleth diagrams of $O_{3\,max}$ were output by the advection-reaction model for 50×50 cases of NO_x and VOC initial concentrations (NO_{x0}, VOC_0). The $O_{3\,max}$ isopleth diagrams for meteorological conditions in the 95–100th percentile rank interval of the TMA ozone level are shown in Fig. 8a and b for D=3 and 6 h. On the diagrams, the line connecting maximum $O_{3\,max}$ values for each VOC_0 (the "ridge line") is defined as the boundary between the VOC-limited regime (above the line) and the NO_x-limited regime (below the line). This boundary is approximately linear and extrapolates to the origin. Importantly, for each normalized distance, the isopleth diagram shows two clear ozone formation regimes. The cause of the formation of two regimes for $O_{3\,max}$ at each normalized distance D is discussed in Sect. 4. The regime boundary moves as the normalized distance D increases and, consequently, the regime in which a given VOC/NO_x initial condition falls may also change with D. Importantly, as D increases, the NO_x-limited regime occupies a larger area of the diagrams, reflecting the increase in the time of exposure to solar radiation necessary for photochemical reaction and the

ACPD
9, 12927–12963, 2009

resulting increase in $O_{3\,max}$ discussed in detail in Sect. 4.1. As a result, the initial NO_x concentration that results in the highest $O_{3\,max}$ for an arbitrary value of VOC_0 increases continuously with D (Fig. 9). As shown in Fig. 9, the rate of increase of $O_{3\,max}$ with D in the VOC-limited regime near the boundary is high, but in the NO_x-limited regime, apart from the boundary, the rate of increase of $O_{3\,max}$ with D becomes low.

3.3 Spatial reversals of the ozone weekend effect

Points A and B in Fig. 8a and b are examples of initial concentrations of precursors. Point A is at NO_{x0}=60 ppb and VOC_0=480 ppbC (typical morning concentrations in coastal urban areas, and VOC/NO_x=8, which is the same as the mean weekday ratio for the 95–100th percentile rank interval in the TMA). Point B was determined by reducing NO_{x0} by 45% and VOC_0 by 22.5% relative to the values at point A (these reduction rates are similar to those that occur on Sundays; see Fig. 1), and VOC/NO_x is ∼11.3. Point A is still in the VOC-limited regime at D=6 h, but point B is in the NO_x-limited regime at that distance. As a result, at D=3 h, points A and B are both in the VOC-limited regime and $O_{3\,max}$ is higher at point B than at point A, because the depletion of NO_x inhibition for ozone formation exceeds the depletion of ozone formation by VOC reduction. However, at D=6 h, the lower NO_x input causes $O_{3\,max}$ at point B, in the NO_x-limited regime, to be lower than at point A. Tracing of $O_{3\,max}$ along the transport path from the initial precursor concentration of point A and B (Fig. 8c) show a reversal of the ozone weekend effect with distance D from the source, reproducing the observed results shown in Fig. 3d. Figure 8d shows the arrival time of the air mass bringing the daily maximum ozone concentration (T_{max}) in relation to D. Of course, T_{max} increases with D. Moreover, T_{max} for the initial precursor concentrations indicated by point B, which is closer to the NO_x-limited regime than point A, is later than T_{max} for those of point A, probably because conditions become more suitable for ozone formation as the highest daytime temperatures occur after noon.

ACPD
9, 12927–12963, 2009

3.4 Reversals of the ozone weekend effect in relation to meteorological conditions

Factors governing the changes in the ozone isopleth diagram at an arbitrary distance *D* include the meteorological conditions as well as the reactivity of the VOC composition. We compared the regime boundaries calculated by the advection-reaction model between meteorological conditions indicated by the 75–80th percentile rank interval of the TMA ozone level (Fig. 7) and those indicated by the 95–100th percentile rank interval (Table 2), but using the VOC compositions of the 95–100th percentile interval for both. Under less suitable meteorological conditions for ozone formation, the evolving speed of the NO_x-limited regime with distance from the source is lower than that under highly suitable meteorological conditions for ozone formation. Therefore, a longer time (i.e., a longer distance from the source) is required for the change to the NO_x-limited regime. This directly accounts for the observation that the reversal of the ozone weekend effect occurs at more remote points from the source under less suitable meteorological conditions for ozone formation, as shown in Fig. 3a–d. The relationship between the change in meteorological conditions and the reversal point of the ozone weekend effect is diagrammed in Fig. 10 for the initial precursor concentrations A (weekday) and B (Sunday) (see Fig. 8). The reversal point shifts to more remote points as the meteorological conditions become less suitable (lower percentile rank intervals). Finally, under the conditions of the 65–70th percentile (or less) rank interval, reversal cannot occur within a single day. Thus, for reversal of the ozone weekend effect to occur, meteorological conditions must be more suitable than some critical level. Though the reversal point may also be changed by the assumed initial weekday and Sunday concentrations, Fig. 10 clearly shows that a fundamental relationship exists between meteorological conditions and the reversal point of the ozone weekend effect. It is notable that when the reversal occurs, the regime boundary is closer to the Sunday initial VOC/NO_x ratio than to the weekday ratio (Fig. 10). The implications of this are discussed in Sect. 4.3.

ACPD

9, 12927–12963, 2009

4 Discussion

4.1 Change of the ozone formation regimes

The advection-reaction model, by focusing on daily maximum ozone concentrations at a point in a Eulerian coordinate system, clarifies the effect of the restriction of solar energy, which is necessary for the photochemical reactions, caused by distance from the precursor source. According to this model, increases in the amount of solar energy bring not only higher $O_{3\,max}$ but also expand the area of the NO_x-limited regime on isopleth diagrams.

It is well known that conditions in an air mass change from a VOC-limited to a NO_x-limited regime during the chemical transport process (e.g., Sillman, 1999). HO_x radical chain (OH-RO_2-RO-HO_2-OH) reactions are important reactions that increase the ozone concentration. They terminate mainly by peroxy radical reactions in an NO_x-limited regime (Reactions R1, R2), or by OH consumption by reaction with NO_2 in a VOC-limited regime (Reaction R3) (Jacob, 1999; Sillman, 1999; Jenkin and Clemitshaw, 2000).

$$HO_2 + HO_2 \rightarrow H_2O_2 + O_2 \quad \text{(R1)}$$

$$RO_2 + HO_2 \rightarrow ROOH + O_2 \quad \text{(R2)}$$

$$OH + NO_2 \rightarrow HNO_3 \quad \text{(R3)}$$

At a relatively early stage in the photochemical process when NO_x is abundant, Reaction (R3) is a more important termination process than Reactions (R1) and (R2); therefore, incremental increases in NO_x tend to inhibit ozone formation. However, because reaction (R3) eliminates NO_x from the system, the relative importance of Reactions (R1) and (R2) gradually increases. This change causes the change to an NO_x-limited regime in an air mass.

The $O_{3\,max}$ regime change with distance D calculated by the advection-reaction model occurs in different air masses, but it is similar to the regime change in a single air

ACPD
9, 12927–12963, 2009

mass as shown below. The relative contribution of the peroxy radicals (Reactions R1, R2) to OH consumption, leading to radical chain termination, can be estimated by the following equation.

$$R_{R1} = \{p[H_2O_2] + p[ROOH]\}/p[HNO_3] = \{k_1[HO_2]^2 + k_2[RO_2][HO_2]\}/k_3[NO_2][OH], \quad (1)$$

where k_1, k_2 and k_3 are the rate constants of Reaction (R1)~(R3), and "$p[x]$" denotes a production rate of x.

Percentage changes in the OH, NO_2, HO_2 and RO_2 (universal peroxy radical operator in CBIV) concentrations from D=3 h to D=4 h are shown in Fig. 11 as isopleth diagrams. The changes shown in these panels were analytically estimated between different air masses. Near the boundary of the VOC-limited regime, the HO_2 and RO_2 concentrations show large increases, in contrast to small decreases in the OH and NO_2 concentrations. The consequent increase of R_{R1} in accordance with Eq. (1) in the proximity of the regime boundary increases the contribution of Reactions (R1) and (R2) to radical chain termination similarly with processes in a single air mass, causing the expansion of the NO_x-limited regime to encompass the lower initial VOC/NO_x area.

The regime boundary shift and the accompanying increase of $O_{3\,max}$ on the boundary (Fig. 9) indicate that within the VOC-limited regime, more solar radiation will lead to further photochemical reactions, whereas within the highly NO_x-limited regime, the reactions are terminated once most of the NO_x has been consumed.

The shift of the regime boundary depends mainly on three parameters: (1) the total energy of solar radiation received during the advection from the source, (2) the intensity of the solar radiation, and (3) VOC reactivity. We have already shown the effects of the first and second parameters. We show the effect of the third parameter in the following example. First we prepared $O_{3\,max}$ isopleths for individual CBIV species groups by the advection-reaction model for D=6 h, and then we compared the regime boundaries, and $O_{3\,max}$ concentrations along the boundary for two VOC initial concentrations (Table 3). Ozone concentration on the regime boundary is important because it indicates

ACPD
9, 12927–12963, 2009

capable highest ozone level at a given VOC_0. Highly reactive species such as ISOP and OLE show lower regime boundaries and higher O_3 concentrations on the boundary; with exceptions such as ETH, having larger boundary but higher $O_{3\,max}$ on the boundary. It is interesting that the arriving time of the air mass which brings the $O_{3\,max}$ on the boundary for formaldehyde (FORM) is specifically later than other species. This is caused by the late arrival of the O_3 rich air mass, which has the highest HO_2 production efficiency by the formaldehyde photolysis due to the highest solar radiation around noon at the relatively early stage of reaction. Reactivity of TMA VOC composition, attached in Table 3, reflects the lowest reactivity of the abundant PAR in the air shown in Table 1.

Temperature is also thought to modify the speed of shift of the regime boundary, with variable effect according to the VOC species, but for simplicity we do not address this here.

An attainable minimum regime boundary within a single day's transport is an important index as well as a speed of shifting regime boundary; which means a minimum VOC/NO_x initial concentrations ratio that the air mass can enter into the NO_x-limited regime after the one day transport. Because the substantial emissions in urban area begin after sun rise, the attainable minimum boundary is obtained by the air mass which starts from the upwind edge of source area at that time. The attainable minimum boundary is estimated to be 7.8 under the 95–100 percentile rank ozone meteorological conditions in the case of $L=2$ h (Table 2). For cases of different source sizes, the value (7.7) for $L\rightarrow 0$ case (mostly concentrated source) is similar to that for $L=2$ h. On the other hand, the value (8.4) for $L=4$ h case (extremely distributed source) is slightly higher because the cumulative solar radiation supplied for the photochemical reactions of precursors injected into the air mass is lower than that for the concentrated source. Thus, the attainable minimum regime boundary is affected by the source size as well as the solar intensity and the reactivity of VOCs.

ACPD
9, 12927–12963, 2009

4.2 Applicability of the model to the real world

One of the differences between our simple theoretical model and the real world is that in the latter, diffusion and dry deposition influence the transport process. Diffusion, including dilution by growth of the boundary layer, tends to inhibit increases in the ozone concentration by photochemical reaction. However, if the rates of diffusion of the precursors and of the photochemical products are similar, the ozone isopleth diagram will retain its basis feature. However, because dry deposition of NO_2 accelerates the elimination of NO_x from the atmosphere, dry deposition probably tends to cause a more rapid shift of the regime boundary. As a result, reversals of the ozone weekend effect would be more easily observable.

Spatial and temporal variations in wind direction and speed tend to disturb the $O_{3\,max}$ distribution. However, air masses arriving at points more remote from the source experience a stochastically longer reaction time, and therefore receive more solar radiation during transport; consequently, they tend to be more NO_x-limited. This supports the observation that the reversal of the ozone weekend effect occurs more frequently at more remote points.

A complex spatial distribution of precursor sources may greatly affect the $O_{3\,max}$ distribution and likely leads to ambiguous ozone weekend changes. The simple advection–reaction model cannot deal with such complexities. However, in the case of the presence of spatial large changes of emission density shown in Fig. 3e and f, our model may have a capability of understanding of the fundamental structure in ozone weekend effect and its reversal.

In accordance with the model property mentioned above, it is plausible that the reversal of the ozone weekend effect occurs according to the principle elucidated by the advection-reaction model. Several studies using three-dimensional numerical chemical transport models have found a change in the ozone formation regime along the transport path (Milford et al., 1994; Sillman, 1999; Carmichael et al., 2003; Beekmann and Vautard, 2009). For example, Carmichael et al. (2003) reported that the ozone forma-

ACPD
9, 12927–12963, 2009

tion regime changes from VOC-limited to NO_x-limited along the transport path, on the basis of a doubling NO_x numerical experiment in East Asia, and Jiménez et al. (2005) reported a change in the ozone weekend effect along the transport path on the basis of a numerical simulation for the northeastern Iberian Peninsula. The essential cause of the change in the ozone formation regime and/or the reversal of the ozone weekend effect found by these modeling studies can be expressed by the simple advection-reaction model described in this paper, in particular in relation to the increased amount of solar radiation exposure necessary for the photochemical reactions with distance from the emission source.

One of the important results of this study is the fact that the release time of the air mass that brings the highest ozone concentration to a distance *D* from the source (Table 2) is earlier in the day for more remote points compared with points closer to the source. This is important information for the development of countermeasures to ozone pollution such as activity controls in urban areas.

4.3 Judgment of ozone formation regime by observation

As shown by the above discussion, the $O_{3\,max}$ formation regime continuously varies with (1) distance from the precursor source, (2) meteorological conditions, and (3) reactivity of the emitted VOCs and VOC/NO_x. We believe that the observed reversals of the ozone weekend effect occur as a result of the regime change from weekday to weekend caused by the change in the initial VOC/NO_x ratio. The estimated values of several parameters in the Tokyo metropolitan area (TMA) are summarized in Table 4. If the observed morning VOC/NO_x in the TMA coastal urban center (CUC) is taken as the initial condition, a regime boundary where the reversal of the weekend effect is observed can be estimated by the weighted mean value of these initial conditions on weekdays and weekends (from Fig. 10; see also Fig. 4b): 10.5 at the 98th percentile rank and 8.4 at the 80th percentile rank. Roughly estimated distances from the CUC to the inland reversal point of the ozone weekend effect are about 30 km at the 98th percentile rank and about 60 km at the 80th percentile rank, as shown in Fig. 3d and b (ca.

ACPD
9, 12927–12963, 2009

3 and 6 h of advection time by assuming 3 m/s of wind speed). From these parameters, we can estimate that $O_{3\,max}$ formation at points nearer than 30 km (60 km) from the emission source with an initial VOC/NO_x of ~10.5 (8.4) under extremely suitable, 98th percentile rank (relatively suitable, 80th percentile rank), meteorological conditions is governed by VOC-limited chemistry, but at more distant points, it is governed by NO_x-limited chemistry. It should be noted that the above inference is made for specified meteorological conditions and a specified initial VOC/NO_x ratio.

In the Osaka-Kyoto area (Fig. 3), the reversal points are apparently nearer to the CUC than in the TMA. Though we have not yet investigated the reason for this difference, a relatively higher solar intensity (ca. 10% higher than in the TMA) is one of the possible reasons for the more rapid regime change. Though there are many factors that modify the ozone formation regime in the real world, as stated in the preceding section, reversal observation is one method that can be used to judge ozone formation regimes in further research work.

5 Summary

Over broad areas of Japan, extremely systematic reversals of the ozone weekend effect are observed in hourly data monitored at many observation sites. The important features are (1) spatial reversals from a weekend increase in the vicinity of huge precursor source areas to a weekend decrease in the surrounding rural areas, and (2) temporal reversals from a weekend increase under relatively unsuitable meteorological conditions for ozone formation to a weekend decrease under relatively suitable conditions.

Using a simple advection-reaction model, we estimated the cause of the reversals of the ozone weekend effect to be a shift in the regime boundary in an air mass bringing $O_{3\,max}$ with distance from the precursor source, with a larger reduction rate of NO_x weekend emissions than VOC emissions as a necessary condition.

Ozone weekend changes depend on solar intensity as well as on the VOC/NO_x ratio

ACPD
9, 12927–12963, 2009

of emissions. Daily cumulative solar radiation in the 95–100th percentile rank interval of the TMA ozone level is 21.5 MJ/m^2 (Fig. 7, TMA is at 35° N). Big cities and their surrounding areas anywhere in the world that experience similar solar intensity to that of the TMA, and where human activities change at the weekend, may show a similar reversal of the ozone weekend effect. For detection of ozone weekend changes, comparison between weekdays and weekends at the same percentile rank of ozone concentration is a simple and useful method because it allows comparison under similar meteorological conditions.

Furthermore, considering the theoretical findings described above, we can determine the ozone formation regime for the daily maximum ozone concentration at a specific location under specific meteorological conditions by observing ozone weekend changes.

Acknowledgements. This work was supported by the cooperative research project ("Study on characteristics of photochemical oxidants and particulate matter") of the National Institute for Environmental Studies and the local governmental institutes for environmental research in Japan. We would like to acknowledge all the staff of this project.

References

Altshuler, S. L., Arcado, T. D. and Lawson, P. K.: Weekday vs. weekend ambient ozone concentrations: Discussion and hypotheses with focus on Northern California, J. Air Waste Manage., 45, 967–972, 1995.

Beekmann, M. and Vautard, R.: A modelling study of photochemical regimes over Europe: robustness and variability, Atmos. Chem. Phys. Discuss., 9, 1521–1560, 2009, http://www.atmos-chem-phys-discuss.net/9/1521/2009/.

Blanchard, C. L. and Fairley, D.: Spatial mapping of VOC and NO_x-limitation of ozone formation in central California, Atmos. Environ., 35, 3861–3873, 2001.

Brönnimann, S. and Neu, U.: Weekend-weekday differences of near-surface ozone concentrations in Switzerland for different meteorological conditions, Atmos. Environ., 31, 1127–1135, 1997.

Carmichael, G. R., Tang, Y., Kurata, G., et al.: Regional-scale chemical transport modeling in support of observations obtained during the TRACE-P experiment, J. Geophys. Res., 108(D21), 8823, doi:10.1029/2002JD003117, 2003.
Carter, W. P. A., Winer, A. M., and Pitts Jr., J. N.: Effects of kinetic mechanisms and hydrocarbon composition on oxidant-precursor relations predicted by the EKMA isopleth technique, Atmos. Environ., 16, 113–120, 1982.
Cleveland, W. S., Graedel, T. E., Kleiner, B., and Warmer, J. L.: Sunday and workday variations in the photochemical air pollution in New Jersey and New York, Science, 186, 1037–1038, 1974.
Elkus, B. and Wilson, K. R.: Photochemical air pollution: weekend-weekday differences, Atmos. Environ., 11, 509–515, 1977.
Fujita, E. M., Stockwell, W. R., Campbell, D. E., Keislar, R. E., and Lawson, D. R.: Evolution of the magnitude and spatial extent of the weekend ozone effect in California's South Coast Air Basin, J. Air Waste Manage., 53, 802–815, 2003.
Gery, M. W., Whitten, G. Z., Killus, J. P., and Dodge, M. C.: A photochemical kinetics mechanism for urban and regional scale computer modeling, J. Geophys. Res, 94, 12925–12956, 1989.
Heuss, J. M., Kahlbaum, D. F., and Wolff, G. T.: Weekday/weekend ozone differences: what can we learn from them?, J. Air Waste Manage., 53, 772–788, 2003.
Jacob, D. J.: Introduction to atmospheric chemistry, Princeton University Press, 1999.
Jenkin, M. E. and Clemitshaw, K. C.: Ozone and other secondary photochemical pollutants: chemical processes governing their formation in the planetary boundary layer, Atmos. Environ., 34, 2499–2527, 2000.
Jiménez, P., Parra, R., Gassó, S., and Baldasano, J. M.: Modeling the ozone weekend effect in very complex terrains: a case study in the Northeastern Iberian Peninsula, Atmos. Environ., 39, 429–444, 2005.
Kannari, A.: An analysis of weekend effects on photochemical oxidant concentrations in the Kanto and Kansai regions, Part 1 Finding of two kinds of reversals on weekend effect, J. Jpn. Soc. Atmos. Environ., 41(4), 209–219, 2006a (in Japanese with English abstract).
Kannari, A.: An analysis of weekend effects on photochemical oxidant concentrations in the Kanto and Kansai regions, Part 2 Verification of dynamically changing ozone formation regimes, J. Jpn. Soc. Atmos. Environ. 41(4), 220–233, (in Japanese with English abstract) 2006b.

ACPD
9, 12927–12963, 2009

Kannari, A. and Ohara, T.: A mechanism of reversals on the ozone weekend effect, J. Jpn. Soc. Atmos. Environ., 44(2), 82–90 (in Japanese with English abstract), 2009.

Kannari A., Tonooka, Y., Baba, T., and Murano, K.: Development of multiple-species 1 km×1 km resolution hourly basis emissions inventory for Japan, Atmos. Environ., 41, 3428–3439, 2007.

Milford, J. B., Gao, D., Sillman, S., Blossey, P., and Russel, A. G.: Total reactive nitrogen (NO_y) as an indicator of the sensitivity of ozone to reductions in hydrocarbon and NO_x emissions, J. Geophys. Res., 99(D2), 3533–3542, 1994.

Murphy, J. G., Day, D. A., Cleary, P. A., Wooldridge, P. J., Millet, D. B., Goldstein, A. H., and Cohen, R. C.: The weekend effect within and downwind of Sacramento: Part 2. Observational evidence for chemical and dynamical contributions, Atmos. Chem. Phys. Discuss., 6, 11971–12019, 2006, http://www.atmos-chem-phys-discuss.net/6/11971/2006/.

Paschalidou, A. K. and Kassomenos, P. A.: Comparison of air pollutant concentrations between weekdays and weekends in Athens, Greece for various meteorological conditions, Environ. Technol., 25, 1241–1255, 2004.

Pun, B. K. and Seigneur, C.: Day-of-week behavior of atmospheric ozone in three U.S. cities, J. Air Waste Manage., 53, 789–801, 2003.

Sillman, S.: The relation between ozone, NO_x and hydrocarbons in urban and polluted rural environments, Atmos. Environ., 33, 1821–1845, 1999.

Stephens, S., Madronich, S., Wu, F., Olson, J. B., Ramos, R., Retama, A., and Muñoz, R.: Weekly patterns of México City's surface concentrations of CO, NO_x, PM_{10} and O_3 during 1986–2007, Atmos. Chem. Phys., 8, 5313–5325, 2008, http://www.atmos-chem-phys.net/8/5313/2008/.

Table 1. Estimated VOC composition of emissions during 05:00–15:00 LT in July in the TMA.

CBIV species groups	Volume %
PAR (paraffin carbon bond)	81.77
ETH (ethene)	1.06
OLE (olefinic carbon bond)	1.66
TOL (toluene)	2.67
XYL (xylene)	2.12
FORM (formaldehyde)	1.37
ALD2 (high molecular weight aldehydes)	2.13
ISOP (isoprene)	2.62
NR (non-reactive)	4.59

ACPD

9, 12927–12963, 2009

Table 2. Comparison of boundary VOC/NO_x ratio (ppbC/ppb) on the ozone isopleths under different ozone formation conditions.

Normalized distance (h)	Boundary VOC/NO_x (75–80 percentile rank)	Boundary VOC/NO_x (95–100 percentile rank)	Released time[a] (LT) (95–100 percentile rank)[b]	Arrived time[a] (LT) (95–100 percentile rank)[b]
2	43.0	30.6	11.0	13.0±0.0
3	26.4	18.8	10.4	13.4±0.1
4	18.6	13.6	9.9	13.9±0.1
5	15.0	11.1	9.3	14.3±0.1
6	12.9	9.7	8.8	14.8±0.1
7	11.8	8.9	8.3	15.3±0.2
8	11.1	8.4	7.8	15.8±0.2
9	10.7	8.0	7.3	16.3±0.2
10	10.4	7.9	7.0	17.0±0.1
11	10.4	7.9	7.0	18.0±0.0

[a] Mean release and arrival times ± SDs of the air mass bringing $O_{3\,max}$ on the regime boundary.
[b] Release and arrival times under the meteorological conditions for 75–80 percentile rank of $O_{3\,max}$ are similar to those for the 95–100 percentile rank interval.

ACPD
9, 12927–12963, 2009

Table 3. Relative reactivity of CBIV species indicated by the ozone formation regime boundary values and the ozone concentrations at the boundaries. $O_{3\,max}$ isopleths were calculated by the advection-reaction model for D=6 h under the 95–100 percentile rank meteorology shown in Fig. 7.

Rank	CBIV lumped Species	VOC/NO_x[a] Boundary	$O_{3\,max}$ (ppb) on the boundary[b] 100[c]	300[c]	arrival time (LT)[d]
1	ISOP	3.3	142 (30)	310 (91)	15.1±0.1
2	OLE	3.4	150 (29)	310 (88)	15.0±0.2
3	XYL	4.4	85 (23)	180 (68)	14.9±0.2
4	FORM	5.1	90 (20)	225 (59)	15.5±0.1
5	ALD2	5.3	105 (19)	195 (57)	15.0±0.1
6	ETH	8.6	110 (12)	231 (35)	15.0±0.1
TMA VOC composition[e]		*9.7*	*61 (10)*	*127 (31)*	*14.8±0.1*
7	TOL	18.4	15 (5)	55 (16)	14.9±0.2
8	PAR	>100	<10	<10	15.3±0.1

[a] ppbC/ppb.
[b] Numbers in the parentheses indicate NO_{x0} concentrations (ppb) on the boundaries.
[c] VOC_0 concentrations (ppbC).
[d] Mean values ± SDs on the boundary.
[e] See Table 1 and 2.

ACPD
9, 12927–12963, 2009

Table 4. Values of several parameters estimated from observed reversals of the ozone weekend effect in the TMA.

Item		Percentile rank 98th	80th
Observed VOC/NO_x at CUC[a] during 06:00–09:00 LT (ppbC/ppb)	weekdays	8	6
	Sundays	11	9
Observed reversal point of the weekend effect (distance from CUC)[b]		~30 km	~60 km
Advection time from CUC to the reversal point, assuming U=3 m/s		~3 h	~6 h
Estimated regime boundary by the reversal of weekend effect[c] (ppbC/ppb)		~10.5	~8.4
Observed $O_{3\,max}$ at the reversal point		120–140 ppb	80–90 ppb

[a] CUC, Coastal Urban Center.
[b] These values are estimated from Fig. 3b and d.
[c] Mean initial VOC/NO_x weighted by 0.8 for Sunday and 0.2 for weekday, as suggested by Fig. 10.

ACPD
9, 12927–12963, 2009

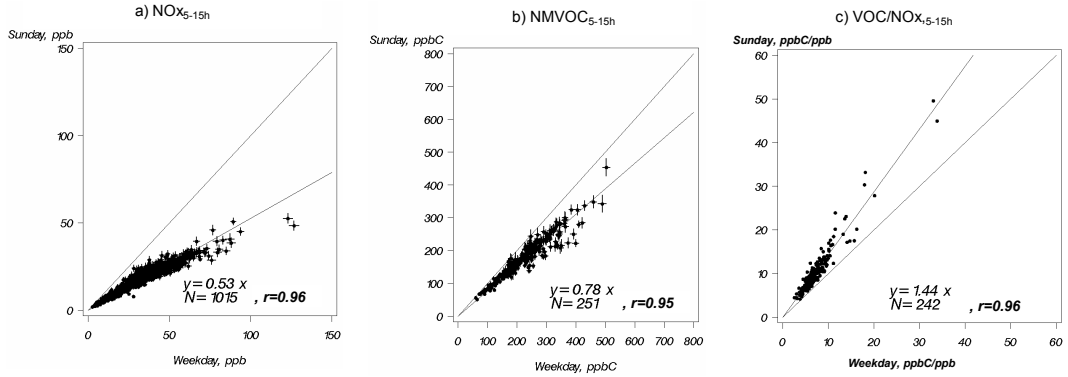

Fig. 1. Comparison of precursor concentrations between weekdays and Sundays measured from 05:00 to 15:00 LT during 1999–2004. Bars in **(a)** and **(b)** indicate the 95% confidence limits of the mean values.

ACPD
9, 12927–12963, 2009

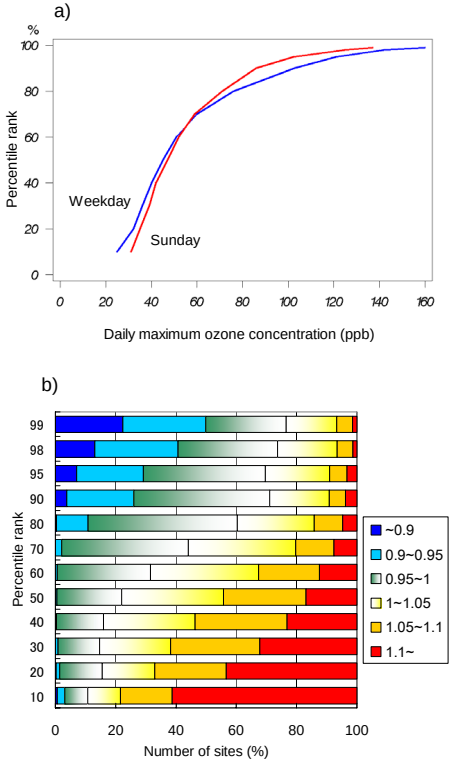

Fig. 2. (a) An example of cumulative frequency curves of daily maximum ozone concentrations for weekdays and Sundays, allowing comparison of values at the same percentile rank. **(b)** Number of sites showing the ozone weekend effect, indicated by the ratio of daily maximum concentrations on Sundays to those on weekdays (colored scale), according to percentile ranking of the ozone concentration. Total number of sites=899, with data available for 1999–2004 in 36 prefectures in mainland Japan (Honshu) and Shikoku and Kyushu islands.

ACPD
9, 12927–12963, 2009

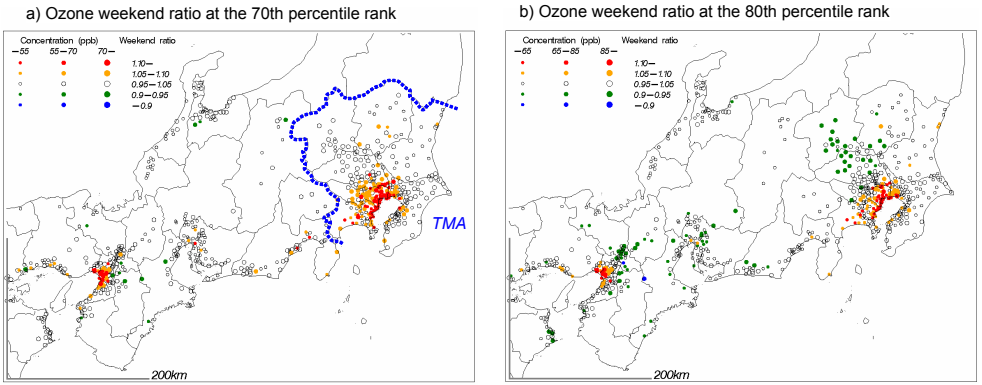

Fig. 3. (a–d) Spatial distributions of ozone weekend ratio on Sundays to weekdays at the (a) 70th, (b) 80th, (c) 90th, and (d) 98th percentile rank. TMA: Tokyo Metropolitan Area. Panels **(e)** and **(f)** show the spatial distributions of mean NO_x and VOC emission fluxes (mg/m^2 per hour) for 06:00–15:00 LT in July 2000 (emission inventory EAGrid2000-JAPAN, Kannari et al., 2007). Biogenic sources are included in the VOC emissions. Tokyo, Nagoya, and Osaka-Kyoto are each at the center of a high emission flux area. The rectangle in the panel **(f)** encloses the target area for estimating the composition of emitted VOCs in Table 1.

ACPD
9, 12927–12963, 2009

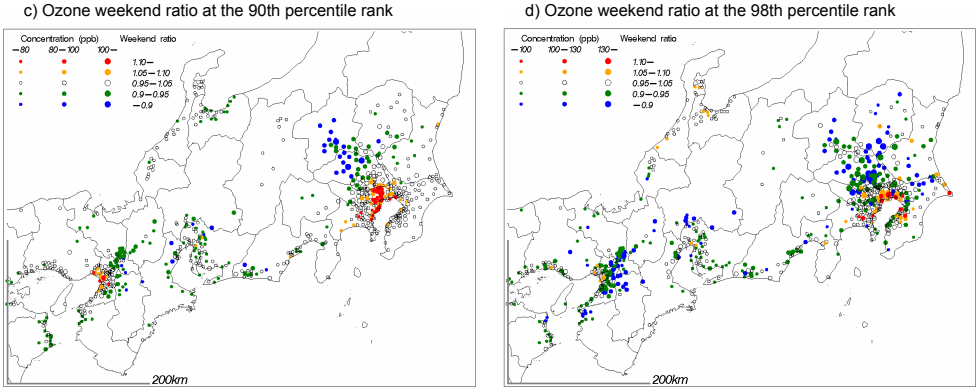

Fig. 3. Continued.

ACPD
9, 12927–12963, 2009

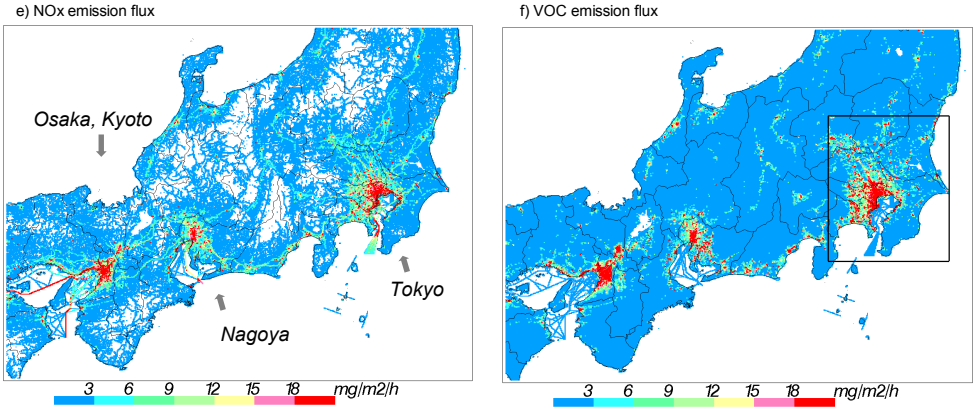

Fig. 3. Continued.

ACPD
9, 12927–12963, 2009

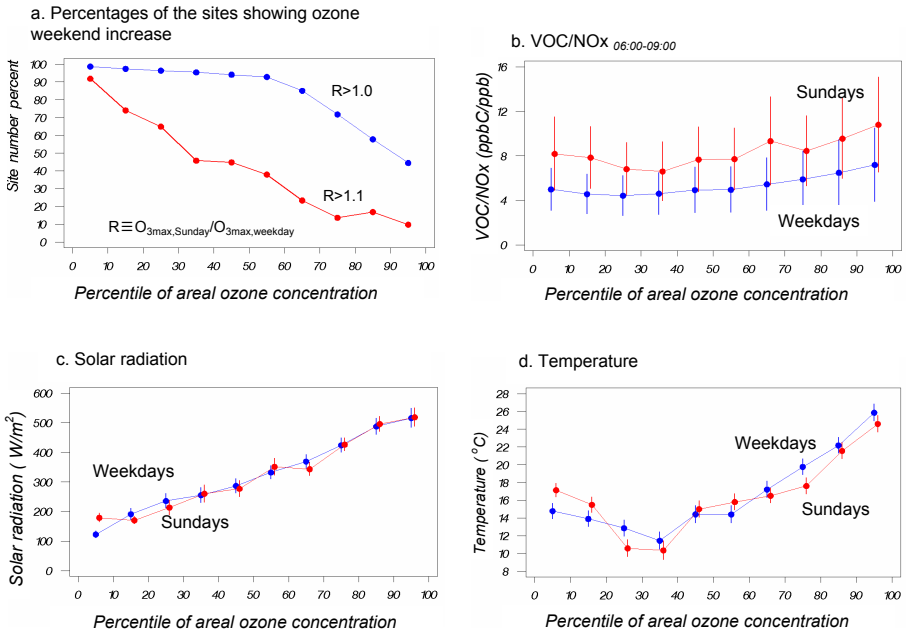

Fig. 4. Variation of parameters with the regional ozone concentration percentile rank in the TMA (see Fig. 3a) in 1999–2004. **(a)** Percentage of sites showing an ozone weekend increase among 308 monitoring sites. **(b)** Mean VOC/NO_x during 06:00–09:00 LT on weekdays and Sundays at 180 monitoring sites. **(c)** Mean solar radiation at 21 monitoring sites. **(d)** Mean temperature at 179 monitoring sites. In (b), (c) and (d), the error bars show the standard deviation (SD).

ACPD
9, 12927–12963, 2009

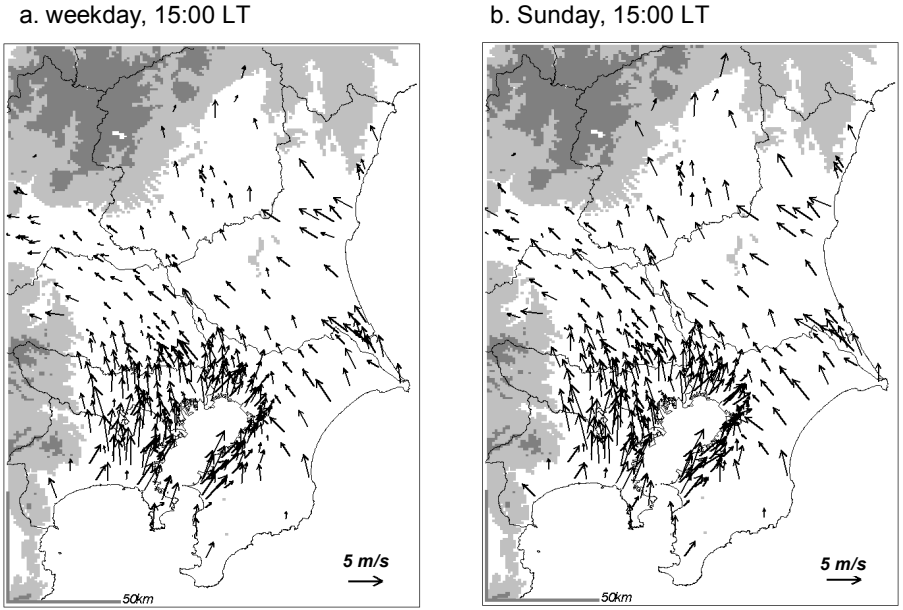

Fig. 5. Mean observed surface wind vectors at 15:00 LT on 95–100 percentile rank days for the TMA ozone level during 1999–2004. Light (dark) gray areas indicate mountainous areas higher than 300 m (1000 m).

ACPD
9, 12927–12963, 2009

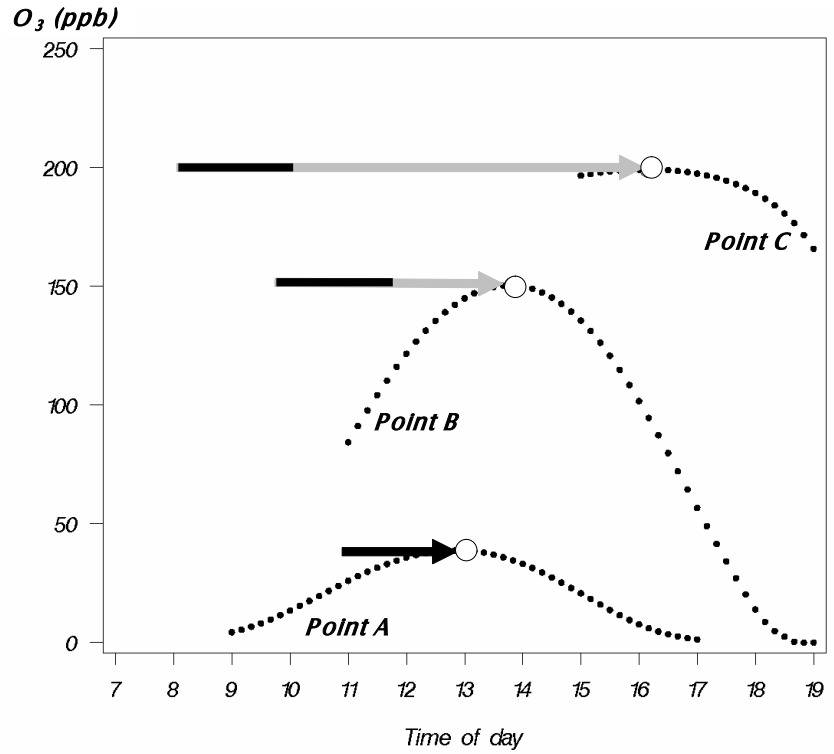

Fig. 6. Schematic diagram of time-dependent O_3 concentrations calculated at point A (near the source, D=2 h), B (middle range, D=4 h), and C (remote, D=8 h), assuming a constant emission rate (beginning at 07:00 LT) and wind speed, and solar radiation and temperature dependent on the time of day. Arrows indicate advection duration of the air mass bringing $O_{3\,max}$. Source length L of precursors is assumed to be 2 h (indicated by the black parts of the arrows).

ACPD
9, 12927–12963, 2009

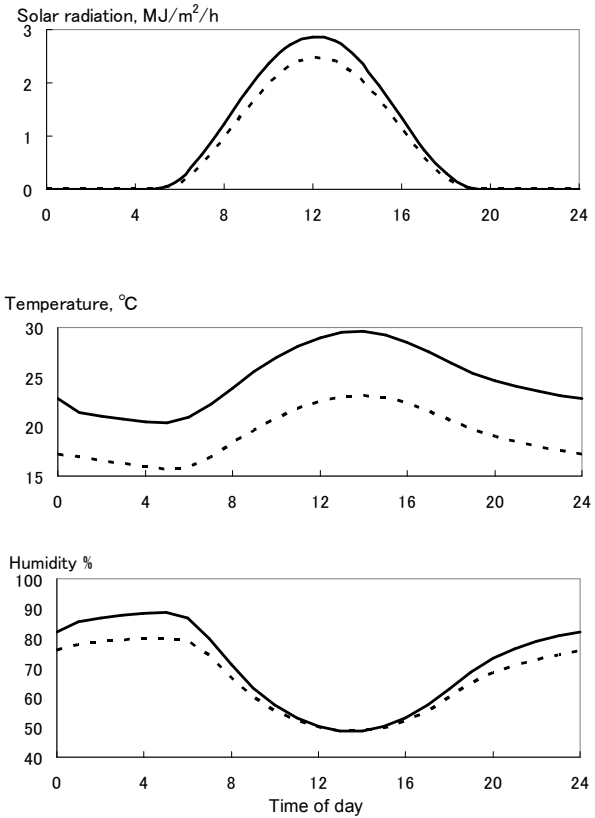

Fig. 7. Mean meteorological conditions for the 95–100th (solid lines) and the 75–80th (dashed lines) percentile rank intervals of $O_{3\,max}$ in the TMA. Values are for weekdays, but those on Sundays are similar. Water vapor concentrations (volume mixing ratios) are nearly constant in daytime (2.1% for the 95–100th, and 1.4% for the 75–80th percentile rank interval).

ACPD
9, 12927–12963, 2009

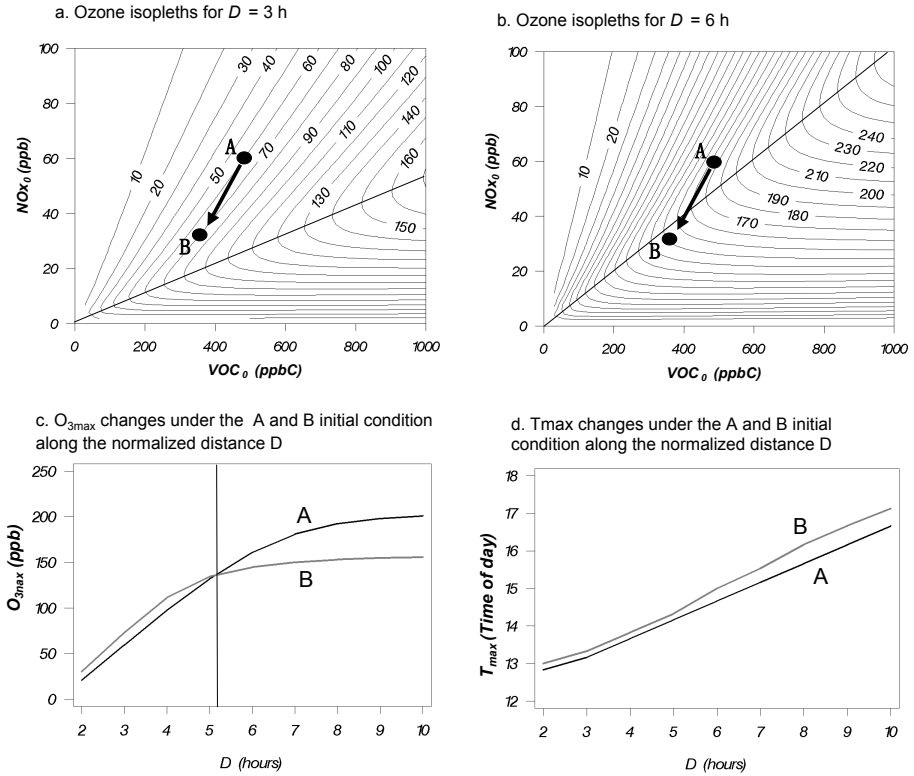

Fig. 8. (a, b) Isopleth diagrams of maximum daily ozone concentrations ($O_{3\,max}$, ppb) calculated by the advection-reaction model for normalized distances D=3 and 6 h under the TMA 95–100 percentile rank ozone meteorological conditions. Source length L is 2 h. Points A and B are examples of initial precursor concentrations. **(c)** Traces of $O_{3\,max}$ and **(d)** occurrence time of $O_{3\,max}$ (T_{max}, time of day) along the normalized distance D for the initial conditions A and B.

ACPD
9, 12927–12963, 2009

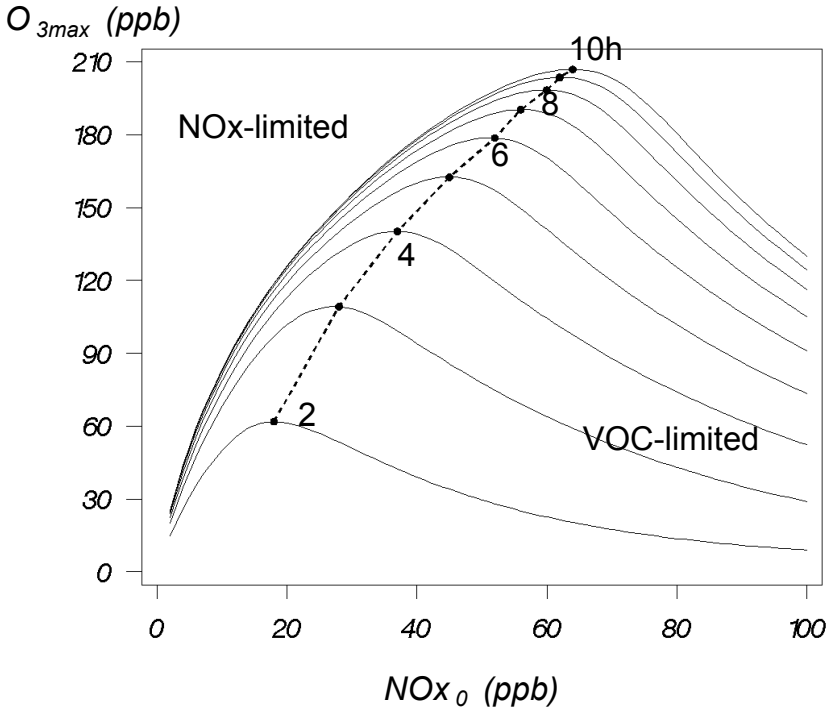

Fig. 9. An example of $O_{3\,max}$ growth and changes of the regime boundary (denoted by the dashed line) with normalized distance D, for an initial NMVOC concentration of 500 ppbC (L = 2 h).

ACPD
9, 12927–12963, 2009

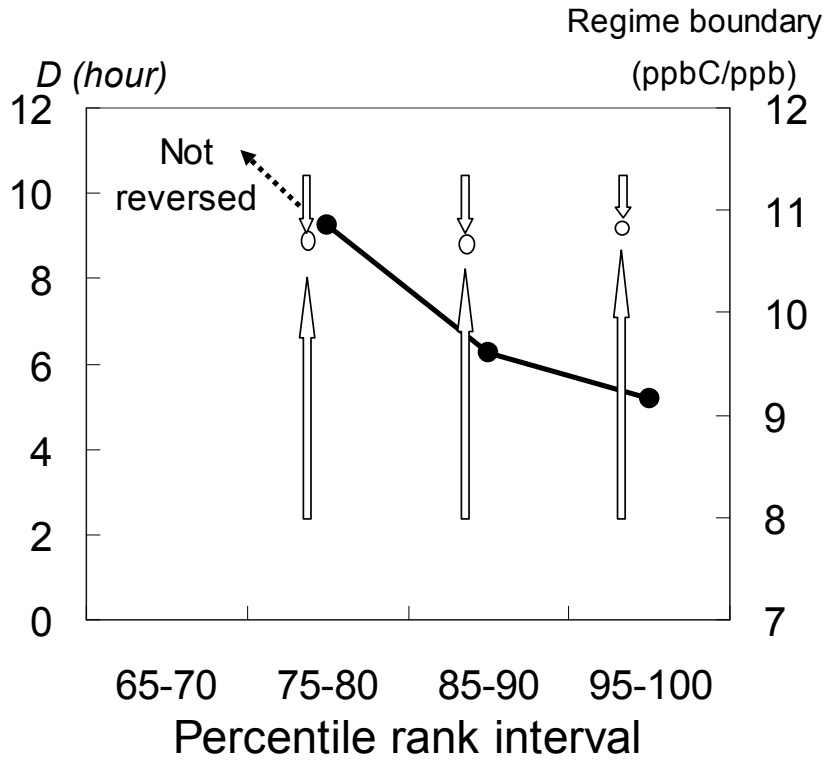

Fig. 10. Changes in the reversal point (black dots and line) of the ozone weekend effect with normalized distance *D*, calculated for various percentile rank intervals meteorology in the TMA, and the regime boundary at the reversal point (open circles). Initial concentrations of VOC and NO_x on weekdays and Sundays are the same as for A and B, respectively, in Fig. 8a and b (VOC/NO_x=8 and 11.3, respectively).

ACPD
9, 12927–12963, 2009

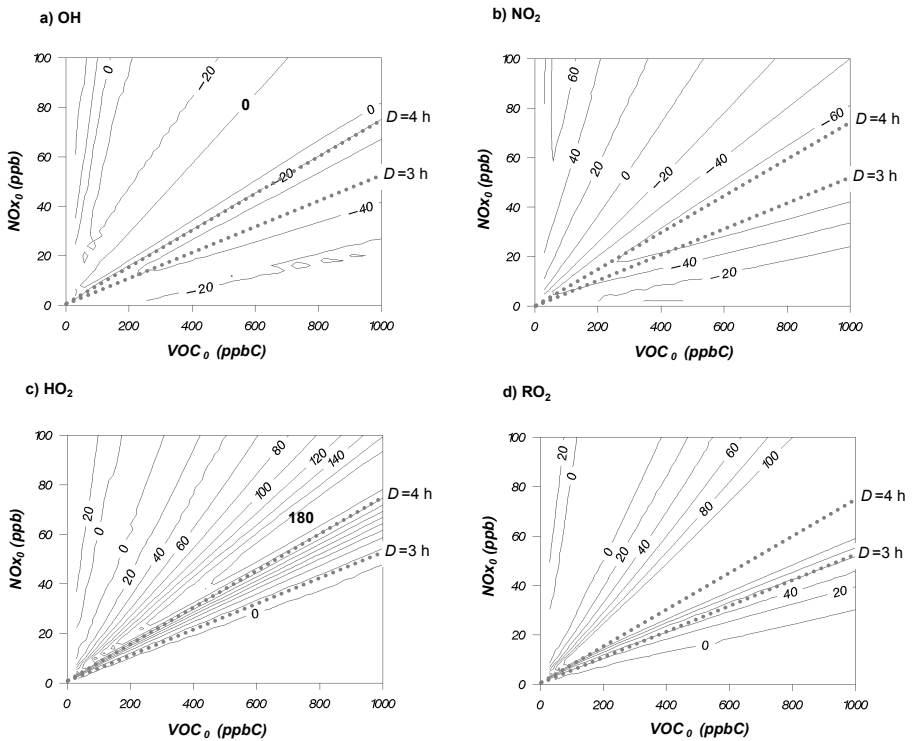

Fig. 11. Isopleth diagrams of the percent changes of OH, NO_2, HO_2, and RO_2 concentrations between D=3 and 4 h. Dashed lines indicate the regime boundaries on the $O_{3\,max}$ isopleth diagrams.

ACPD
9, 12927–12963, 2009